



Sustainable fabric printing by using pre-consumed cellulosic textile wastes: The effect of waste particle content

Zehra Yildiz^{a,*}, Ilyas Kartal^b, E. Dilara Kocak^a, Berivan Ozer^a, Betul Nur Kus^a, Oguz Eryilmaz^a

^a Department of Textile Engineering, Faculty of Technology, Marmara University, Istanbul, Turkey

^b Department of Metallurgical and Materials Engineering, Faculty of Technology, Marmara University, Istanbul, Turkey

ARTICLE INFO

Handling editor: Guoyang Lu

Keywords:

Sustainability
Pre-consumed waste
Screen printing
Cotton fabric
Waste cellulose
Recycling

ABSTRACT

The textile industry generates significant amounts of waste, including yarn/fiber fluffs, fabric scraps, offcuts, etc. These wastes can be recycled and repurposed for usage in screen printing which is a versatile and cost-effective printing technique by producing high-quality prints. In this study, pre-consumed colored cotton wastes were milled into 30–70 μm particle size by using a miller. Then the colored waste particles were included in a commercial printing paste and applied on cotton fabrics via screen printing. Fourier transform infrared (FTIR) spectroscopy, X-ray diffraction (XRD) analysis, and energy dispersive spectrometer (EDS) were employed to observe the chemical changes in the printed textile fabrics. The printed fabrics were evaluated through color, wash/rub fastness, tensile strength, surface wettability, tactile, and air permeability properties. The dispersion quality of the waste particles on textile fabrics was observed by using light microscopy and scanning electron microscopy (SEM) images. The overall results demonstrate that a 10% amount of waste fibrous particle inclusion to the printing paste gave optimum results by means of dispersion quality of wastes, air permeability, and handle properties. Above 10% waste amounts, the waste particles cannot be dissipated well on the fabric surface, resulting in agglomerated and non-uniform printed areas. These findings hold substantial potential for promoting sustainable coloring applications by using colored pre-consumed textile wastes within the textile industry while maintaining high-quality fabric products.

1. Introduction

The textile industry is a significant contributor to the global economy and is known for its rapid pace of production and consumption. However, the industry's environmental impact is significant due to the generation of large amounts of pre-/post-consumer waste and air/water pollution. Recently, the concept of sustainability has gained increasing importance in the textile industry by implementing environmentally friendly practices in the manufacturing of textile-based composites (Eryilmaz et al., 2021, 2023, 2024; Yildiz et al., 2023), and disposal of textiles (Cesar da Silva et al., 2021; Yousef et al., 2020; Tayyab et al., 2020). Pre-consumer waste includes waste generated during the production process, such as fabric scraps, yarn/fiber waste, and offcuts, whereas post-consumer waste includes discarded garments after being used by consumers (Savageau, 2011; Yasin et al., 2019). The disposal of textile waste has significant environmental impacts, contributing to pollution, landfill waste, and greenhouse gas emissions. According to the fast fashion waste statistics of Earth.org, 100 billion garments are

produced each year in the world and 92 million tons of these items are sent to landfills (Igini et al., 2023). Thus, there is a growing demand to find sustainable solutions to manage textile waste.

In the literature, various aspects have been proposed regarding the usage of pre-/post-consumer textile waste for different purposes. One aspect is mechanical recycling, which involves shredding and processing waste textiles into fibers that can be spun into new yarns for fabric production. In this concept, the length of the waste fiber should be within an acceptable range, allowing for efficient blending with other virgin fibers. The other aspect is chemical recycling techniques, such as depolymerization and dissolution, which break down textile waste into its starting monomers, enabling the creation of new fibers, monomers, or oligomers. However, the chemical aspect requires the use of excessive amounts of hazardous solvents and water, leading to new environmental problems and higher production costs (Määttänen et al., 2021; Sheikh et al., 2015; Patti et al., 2020; Yousef et al., 2019). Recently, the mechanical recycling process has been reconsidered, and new solutions have been suggested to reduce waste dimensions to micrometer levels.

* Corresponding author.

E-mail address: zehra.yildiz@marmara.edu.tr (Z. Yildiz).

<https://doi.org/10.1016/j.jclepro.2024.141635>

Received 16 November 2023; Received in revised form 2 February 2024; Accepted 2 March 2024

Available online 9 March 2024

0959-6526/© 2024 Elsevier Ltd. All rights reserved.

For instance, dyed wool waste has been converted into wool powder using a mechanical pulverization process. Subsequently, the waste wool particles have been coated on cotton and polyester fabrics through ionic interaction and pad-dry-cure methods for use as an odor/gas adsorbent and for coloration (Tang et al., 2022a, 2022b). Waste merino wool and alpaca fibers have been mechanically milled using a wet attritor, spray dryer, and air-jet milling processes, and their fine powder properties, such as surface area, rheology, bulk density, etc., have been examined (Rajkhowa et al., 2012; Al Faruque et al., 2019). The waste wool powder was obtained by using a spray-dry method, dissolved in an alkaline solvent, and included in polyacrylonitrile dope solutions to produce PAN/wool wet-spun hybrid fibers. These hybrid fibers were subsequently coated with graphene oxide and used in electrically conductive smart textile applications (Al Faruque et al., 2021).

Screen printing is a widely used printing technique in the textile industry, offering several advantages compared to other printing methods, such as the ability to print on a wide range of fabrics, producing high-quality prints with vivid colors, high durability, low cost, simplicity, and versatility. The technique involves creating a stencil of the desired design on a mesh screen, which is then placed on top of the fabric. Printing paste is pressed through the screen onto the fabric using a scraping knife. The paste is then thermally cured to form a permanent design on the fabric, necessitating the cross-linking of acrylate and butadiene-based oligomers on the surface. For sustainable textile production, screen printing provides an excellent option for repurposing colored textile waste by adding waste powders as pigment materials in the printing paste (Kumar et al., 2022). Waste cotton fabric and fibers have been milled into micron-sized powder and functionalized with transition metal oxides for use in screen printing paste for electrically conductive textile manufacturing (Gan, 2021). In another study, magenta-colored waste cotton fabric was milled into powders of various particle sizes. These waste powders were included in a commercial screen-printing paste as colorful pigments. The study examined the powder morphology, printed fabric color, and fastness properties. It was found that waste powders with dimensions of 5 μm were the most efficient colorful pigment alternative based on rub fastness and fabric color (Gan et al., 2021). According to the literature review, mechanically milled colored textile wastes have been screen-printed on various fabric surfaces, focusing primarily on the fastness and mechanical properties of the final product. In this study, cellulosic pre-consumer denim waste in dark blue color was mechanically milled into micron-sized particles, and the resulting waste particles were included in a commercial acrylate and butadiene-based printing paste as colorant pigments. These prepared pastes were applied to cotton fabrics via screen printing. This study differs from previous studies as the effects of waste particle content in the printing paste on the chemical, mechanical, visual, and comfort properties of the cotton fabrics were all searched. Besides, the examination of the effects of waste particles on air permeability, as well as the tactile properties of the fabrics also supports the novelty of this research.

2. Materials and methods

2.1. Materials

Cotton/PET (80/20%) pre-consumed denim wastes were collected from the edges of the weaving loom in a local textile factory. 2/1 twill weave, desized, and bleached cotton fabrics (170 g/m², 30 weft/cm, 42 warp/cm) were supplied from a local manufacturer and used as a printing substrate. Chemicals for the printing paste (fixing agent, synthetic thickener, anti-foaming agent, emulsifier, urea, softener, acrylate, and butadiene-based binders) were all purchased from Setas Chemical Co.

2.2. Preparation and application of the printing paste

The cotton denim wastes were first cut manually into small strips in

30–70 mm dimensions and then were milled into micron levels. Due to the confidentiality of the milling system, the exact milling procedure was not given in this study. In order to obtain dimensional stability of the waste particles, a woven wire sieve with 73 μm mesh size was used. The dimensions of the sieved waste particles were recorded in the range of 30–70 μm . Fig. 1 illustrates the stages of the preparation of stock screen printing paste and screen-printing process. The stock pigment printing paste was prepared according to the chemical manufacturers' commercial recipe by mixing all compounds in a glass beaker in the following order: 80% distilled water and 1.5% synthetic thickener were stirred by a magnetic stirrer for 10 min. Then, an emulsifier (0.3%), anti-foaming agent (0.2%), and urea (2%) were all added and stirred together for another 10 min. Acrylate and butadiene-based binders (6% each) and softener (0.3%) were included in the beaker and stirred for 5 min. Finally, the fixing agent (7%) was added to the stock pigment printing paste and all ingredients were mixed for 3 min.

Printing pastes were prepared by adding various amounts of denim waste particles (0–20%) and defined with various capital letters as shown in Table 1. In order to observe the viscosity increment of the printing pastes, the viscosity of samples A (without waste), C (with 5% waste), and D (with 10% waste) was measured at room temperature using spindle 6 at 20 rpm (Brookfield RVT viscometer) and found to be 7250, 24,300, and 30,800 cps, respectively. After the preparation of the printing paste, a squeegee was employed to spread the paste on the cotton base fabric with an average 45-degree slope via screen printing. To apply the printing paste onto the cotton fabric uniformly, a metal-framed screen with a mesh size of 140 thread/cm was used. The screen-printing paste was fixed on the cotton fabric at 140 °C for 3 min in a fixation oven.

2.3. Characterization

2.3.1. Attenuated Total reflectance-fourier transform infrared spectroscopy (ATR-FTIR)

ATR-FTIR spectrophotometer (PerkinElmer Spectrum-100 ATR FTIR), equipped with a ZnSe ATR crystal with a variable angle accessory, was employed to investigate the chemical characterization of the printed fabrics in 4000–600 cm⁻¹ mid-infrared spectral range.

2.3.2. X-ray diffraction (XRD) analysis

XRD analysis (Bruker-D2 Phaser, operating at 40 mV and 30 mA,

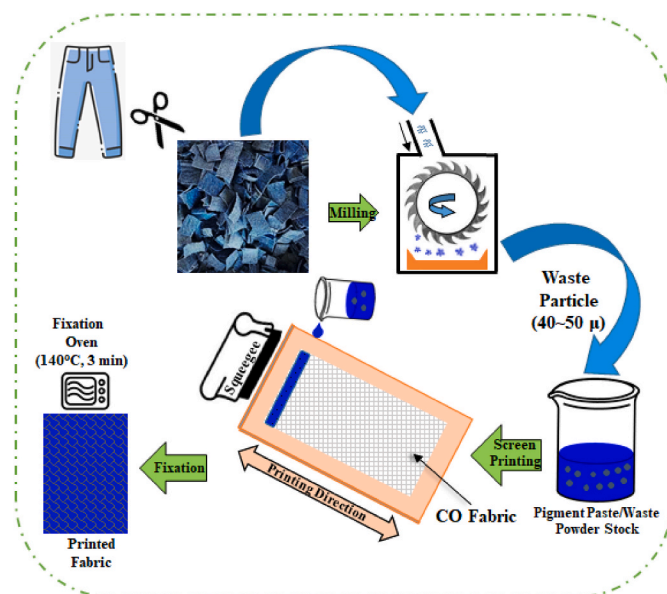


Fig. 1. Workflow of the preparation of stock printing paste and screen-printing process.

Table 1
Fastness and color grades of printed fabrics with various waste particle amounts.

Samples	Waste Particle Cont. (%)	Color Measurement				Wash Fastness (Grade)		Rub Fastness (Grade)	
		L*	a*	b*	K/S _{360 nm} Value	Fade Fastness	Staining Fastness	Dry	Wet
Raw	0	92.48	0.76	5.38	0.22	–	–	–	–
A	0	91.09	0.60	8.01	0.40	5	5	5	5
B	2	81.95	−0.36	4.08	0.55	4	5	5	4
C	5	71.99	−1.12	0.13	0.73	4	5	4–5	3–4
D	10	63.60	−1.43	−2.65	1.02	4–5	5	4	2–3
E	15	60.26	−1.57	−3.57	1.11	4	5	4	2–3
F	20	56.95	−1.56	−4.2	1.28	3	5	3–4	2

across a 2θ range of $10\text{--}40^\circ$ at a rate of $2^\circ/\text{min}$) was used to observe the crystal morphology of the printed fabrics. The crystallinity index (CI) values were calculated by using DIFFRAC.EVA software. A Datacolor SF 600⁺ spectrophotometer was used for measuring the reflectance values of the printed fabrics.

2.3.3. Color measurement

The CIELAB values were calculated by using D65 illuminants and 10° Standard Observer values. During the measurement, the specular component mode and large area view (LAV) 30 mm diameter measuring plate were employed. The color strength values of the printed samples were determined based on the wavelengths of maximum absorption in the visible region, considering the Kubelka-Munk Equation (1) shown below, where R, K, and S represent the reflectance, absorption, and scattering values of the printed fabric at the wavelength of maximum absorption, respectively (Deniz et al., 2022).

$$\frac{K}{S} = \frac{(1 - R)^2}{2R} \quad \text{Eq. 1}$$

2.3.4. Wash/rub fastness testing

The printed fabrics were evaluated through wash fastness in the Gyrowash machine (James H. Heal Co. Ltd) according to the ISO105-C06 (A1S) standard (ISO 105-C06, 2010). The running procedure was set at 40°C for 30 min. Crock-meter (James H. Heal Co. Ltd.) was employed for the rub fastness test according to the ISO 105 X12 standard (ISO 105-X12, 2016). For testing accuracy, each printed fabric was tested three times at different locations and the average results were given.

2.3.5. Contact angle measurement

The surface wettability of the printed fabrics was searched via contact angle measurement by using Gardco PGX + Goniometer with camera equipment by using distilled water droplets with $3\ \mu\text{L}$ volume. The testing condition was set as 10 measurements during 10 s for each droplet.

2.3.6. Tensile testing

The tensile properties of the raw and printed fabrics by means of tensile strength and elongation percentage were investigated by using Instron 4411 tensile testing machine (ISO 13934-1, 2013). Due to the longitudinal screen-printing direction, the tensile test was only applied in the warp direction.

2.3.7. Air permeability testing

The air permeability of the printed fabrics was measured using an air permeability testing device (SDL Atlas) according to the ISO 9237 standard with a $20\ \text{cm}^2$ testing head under 50 Pa air pressure (ISO 9237, 1999).

2.3.8. Evaluation of handle properties

The handle properties of the printed fabrics were assessed using the Tissue Softness Analyzer (TSA) from Emtec Electronic GmbH. This instrument records acoustic signals generated on the fabric surface due to

friction caused by a rotating unit. To ensure precision, five measurements were taken for each sample, and standard deviation (SD) values were provided. All the collected data was processed and analyzed using OriginPro 7.0 software.

2.3.9. Light microscopy and scanning electron microscopy with energy dispersive spectrometer (SEM-EDS)

Polarized DinoLite Digital Microscope AM7013MZT Premier HR with 5-megapixel resolution and scanning electron microscopy along with energy dispersive spectrometer (SEM-EDS) (ZEISS Ltd, JSM-5910LV) were employed to observe the dispersion quality of waste fibrous particles onto the printed fabric surfaces, to measure the length of the waste fibrous particles, and to investigate the changes in elemental composition after screen printing, respectively.

3. Results and discussion

3.1. Chemical characterization

The chemical changes in the cotton fabrics after the screen-printing process were characterized by FTIR spectroscopy, XRD, and EDS analysis. Fig. 2 shows the FTIR spectra of raw fabric, the fabric after the application of only printing paste (A), and the printed fabric with 10 % waste particle (D), respectively. Due to giving better results in further characterization, sample D having 10 % waste particle inclusion was selected for FTIR analysis. The changes in FTIR spectra were mainly created by the chemical compounds in printing paste such as binders, urea, auxiliaries, etc. There was no remarkable change recorded after the inclusion of cellulosic waste particles into the printing paste as the printing substrate was also a cellulosic material (cotton). The characteristic broad hydroxyl ($-\text{OH}$) group peak of cotton fabric was observed in all spectra at 3500 to $3200\ \text{cm}^{-1}$. The existence of urea in the printing paste can be followed by the newly formed peaks in the spectra of A and D such as the N–H stretching peak which overlaps with the $-\text{OH}$ peak at $3300\ \text{cm}^{-1}$, carbonyl stretching peak at $1732\ \text{cm}^{-1}$, N–H bending peak at $1560\ \text{cm}^{-1}$, C–N stretching peak at $1222\ \text{cm}^{-1}$, and other absorbance peak at $1110\ \text{cm}^{-1}$ (Baysal et al., 2019; Kutanaee, 2011). The characteristic peaks of acrylate and butadiene-based binders were observed at 810 and $840\ \text{cm}^{-1}$ (C=C double bond twisting of acrylate), tiny peak at $1632\ \text{cm}^{-1}$ (C=C double bond stretching), and minor peaks at 911 and $968\ \text{cm}^{-1}$ (butadiene), respectively (Wang et al., 2019; Yildiz et al., 2017).

In this study, XRD analysis was employed to search whether the waste particle amount in the printing paste affected the crystallinity of cotton fabrics. Fig. 3 shows the XRD patterns with crystallinity values (%) of raw and printed fabrics for each waste particle amount. The crystallinity values and XRD curves were illustrated in the same order and the arrow on the graph shows the order of crystallinity increment. Accordingly, all samples showed three distinct peaks at 14.8° , 16.5° , and 22.6° , which are characteristic of the cellulose I β structure of cotton (Gan et al., 2021; Nam et al., 2016; Ahmad et al., 2019). After the application of only screen printing paste, in the sample of A, the crystallinity (%) decreased to 62.4 % due to the disruption of tight and stiff

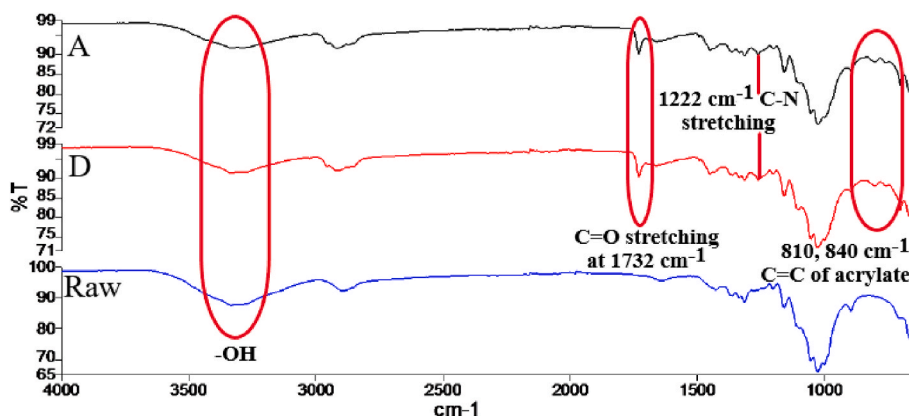


Fig. 2. FTIR spectra of raw and printed fabrics (A and D).

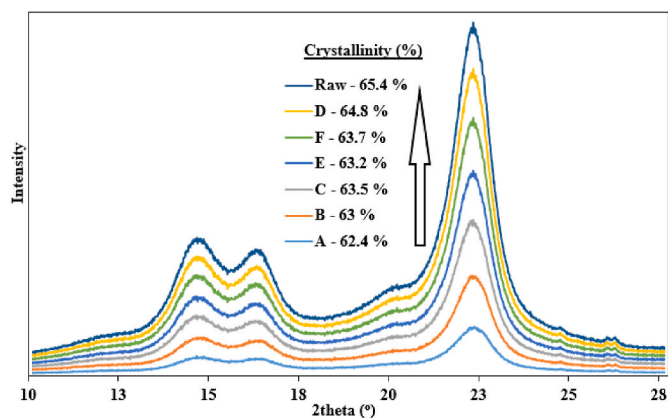


Fig. 3. XRD patterns of raw and printed fabrics.

cellulose crystallites by the effect of branched macromolecules (binder, auxiliaries, etc.), that support the amorphous character, in the printing paste. The crystalline peaks became broad and flat in the sample of A which also supports the existence of a more amorphous nature compared to the raw cotton fabric (O Connell, 2016; Kibasomba et al., 2018). When the cellulosic waste particles were included in the printing paste, through samples B to D, the crystallinity values (%) started to increase. This result can be explained by the crystalline phase of waste particles by itself which helps to increase the overall crystallinity of the printed sample. When the waste particle amount increased above 10 %, in the samples of E and F, the crystallinity values (%) decreased. This result stems from the agglomeration of waste particles in the printing paste resulting in a non-uniform printing layer on the fabric surface. The other reason is the lack of binder amount that does not effectively cover and wet the wastes inside the printing paste. So the excess of waste remains on the screen which cannot be carried through the mesh of the screen.

The raw and printed fabrics were also investigated by means of the elemental composition via EDS analysis. As the cotton fabric composes

of 88–96 % cellulose, 1–1.8 % protein, 0.4–1.2 % pectin, 0.4–1.2 % waxes, 0.8–1.2 % organic acids, 1.5–3.1 % minerals and other impurities, the carbon (C), oxygen (O), and nitrogen (N) elements were recorded and given in Fig. 4. Almost all samples including the raw fabric presented similar N amounts in the range of 5.75–8.33 % due to the existence of protein and minerals in cotton chemical structure. Since all the chemicals in the printing paste and the fibrous waste particles are carbon rich organic substances, it is better to measure the C/O atomic ratio on the elemental analysis of screen printed fabrics (Kumar et al., 2022; Idillovayna, 2023). Accordingly, the raw cotton fabric exhibited C/O atomic ratio of 0.95 whereas this ratio gradually increased through the sample of D and reaches to 2.11. When the fibrous waste amount exceeds 10 %, the C/O atomic ratio started to decrease and the least C/O value of 1.44 was recorded in the sample of F. As mentioned before, this result can be explained by the inefficient dissipation of wastes on the fabric surface due to the lack of binder amount in the printing paste which leads to inadequate covering and wetting of wastes and remaining on the screen.

3.2. Color and wash/rub fastness properties

One of the primary objectives of this study is to explore the feasibility of creating colored textile materials by reusing/repurposing the colored waste particles as pigment materials. In line with this goal, the screen-printed fabrics need to be searched in terms of the color changes against washing and rubbing which is determined by the type and amount of binder (crosslinker) in the printing paste. In this study, common commercially used acrylate and butadiene-based binders were used for covalently bonding the waste particle including printing paste onto the cotton base layer. Table 1, Figs. 5 and 6 summarize the K/S, L*a*b* values, rub/wash fastness grades, and images of printed fabrics along with the solid add on values (%) upon screen printing that were calculated according to a previous study (Tseghai et al., 2020), respectively. Table 1 shows the wash and rub fastness grades of the printed fabrics through the waste particle amounts. Accordingly, all samples showed a great staining fastness property against washing. Whereas the fade fastness decreased a little bit through the sample A to F.

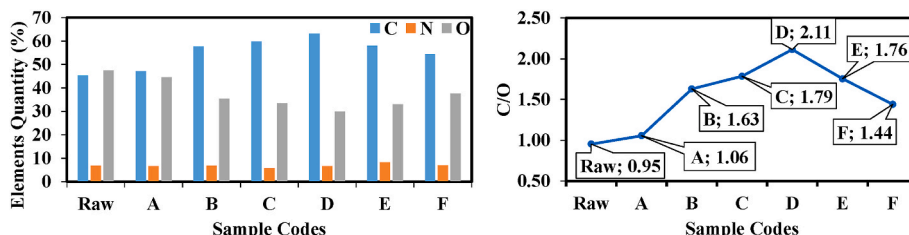


Fig. 4. Elemental composition of raw and printed fabrics along with C/O atomic ratio.

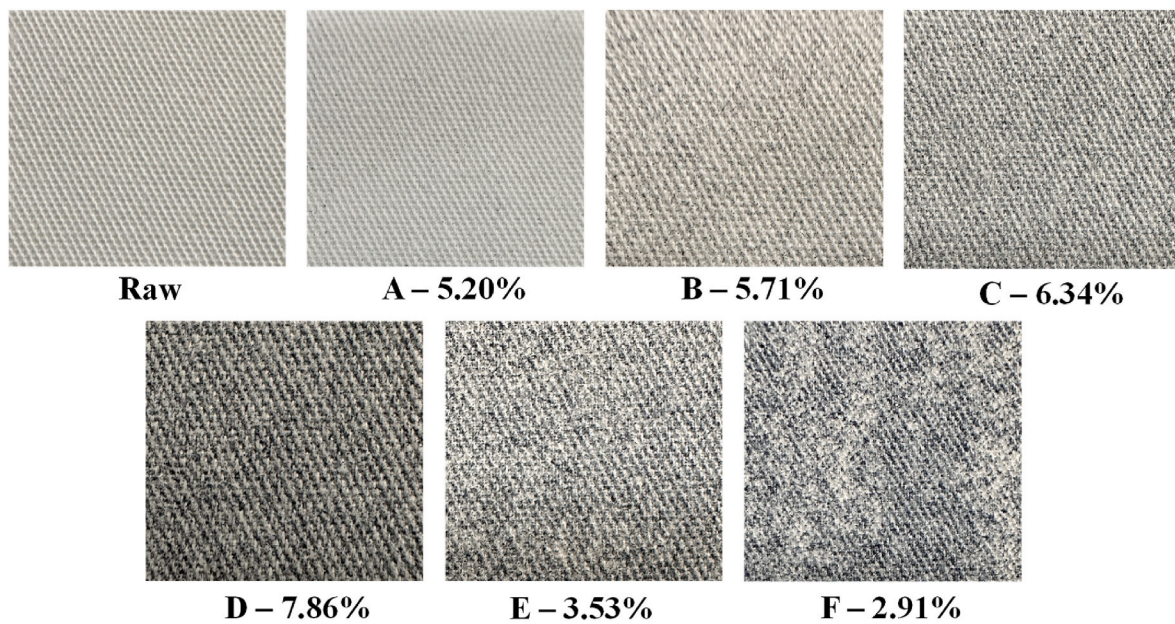


Fig. 5. Images of raw and printed fabrics by means of waste powder content along with solid add-on values.

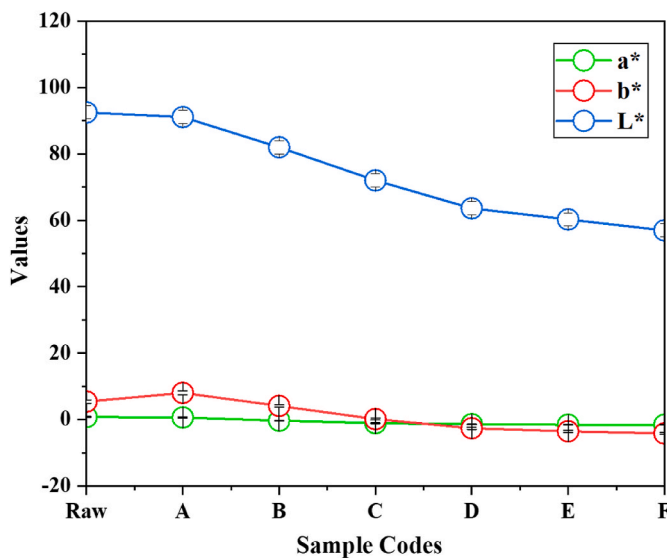


Fig. 6. L*a*b* values of raw and printed fabrics for each waste powder amount.

Considering the ingredients of the printing pastes, there is no waste powder inclusion in sample A thus it is colorless and shows the best fastness grades in both wash and rub fastness tests. After the inclusion of waste particles, the sample of D, which contains 10% waste particle amount, showed the best fade fastness results against washing. The worst fastness great in both washing and rubbing fastness tests was recorded in the sample of F with 20% waste particle inclusion. This result can be explained by the agglomeration of waste particles in printing paste resulting in a non-uniform printed surface as also proven by the fabric images of samples E and F in Fig. 5. Additionally, this may be attributed to the binder amount that is not adequate to cover the waste particle amounts above 10% inclusion (Gan et al., 2021). This explanation can be also supported by using the solid add on values (%) after screen printing process. As expected, the solid add on values were gradually increased with increasing waste particle amount in the printing paste. As a result, the highest solid add on value of 7.86 % was

recorded in the sample of D. Above 10 % waste particle inclusion, the amount of the solid particles deposited on the fabric surface, including the fibrous wastes and printing paste, started to decrease hence the solid add on values decreased in the samples of E and F.

The K/S values of the printed fabrics were recorded in the range of 0.40–1.28. Considering the differences in K/S values, it is obvious that the colored waste particle amount is highly effective on the color strength of printed fabrics. The color of the fabrics became darker through the sample of A to F with increasing colored waste particle amount. According to Table 1 and Fig. 6, the L* values were gradually decreased from sample A to F which means the color became darker with increasing colored waste particle amount. The a* and b* values both refer to the hue changes of the printed samples. When the colored waste particle amount increased, the a* values slightly shifted from a red tone to a greenish color whereas the b* values negatively increased and became closer to the blue color (Yasukawa et al., 2021).

3.3. SEM and light microscopy images

In order to observe the dispersion quality of printing paste and waste fibrous particles, SEM and light microscopy images were employed. Figs. 7–9 show the SEM and light microscopy images of raw and printed fabrics (A, D, F) in 125 × 500×, and 20× magnification, respectively. Sample A shows only the leveling quality of printing paste on the fabric surface as it has no waste particles in that formulation. Considering the other test results, sample D was accepted as the optimum one by means of the waste particle amount whereas sample F was the worst one due to the existence of agglomerated and non-uniform waste particle dissipation on it. Thus, samples D and F were chosen for SEM characterization. Considering the SEM images of raw fabric and sample A, after the application of only printing paste, the paste formulation completely and uniformly covered the fiber surfaces. When the SEM and light microscopy images of samples D and F are compared, it is obvious that a homogeneous and uniform coating and waste particle dispersion quality can be observed in sample D. Whereas, in sample F, the waste particles cannot be dissipated well resulting in agglomeration in some areas as can be seen in Fig. 7 with yellow circles. In order to measure the dimension of waste particles, yellow arrows were used to measure the length of wastes in Fig. 8 D and F. An average waste fibrous particle length was measured in the range of 30–70 μm. Due to the mentioned non-uniform dispersion of wastes in the sample of F, the arrows were

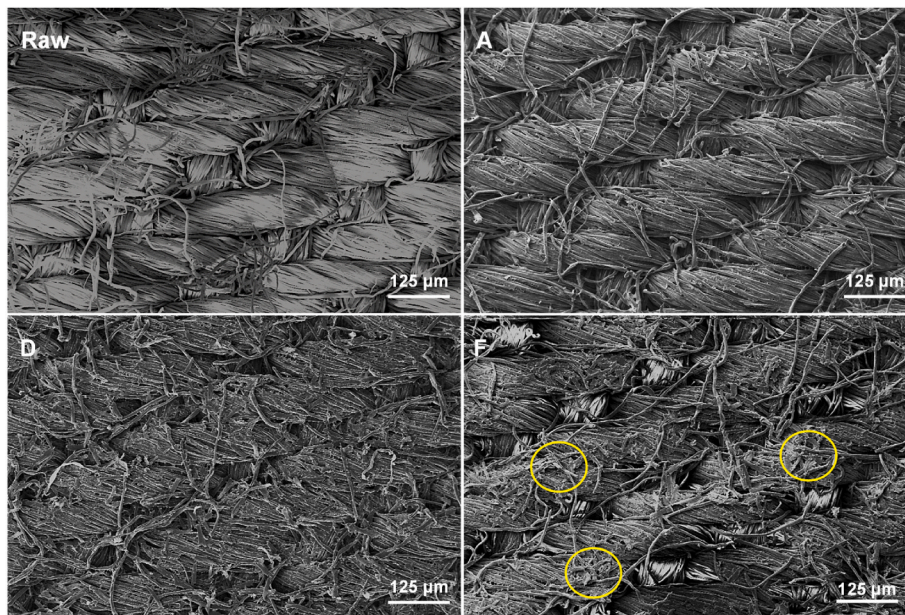


Fig. 7. SEM images of raw and printed fabrics in 125x magnification.

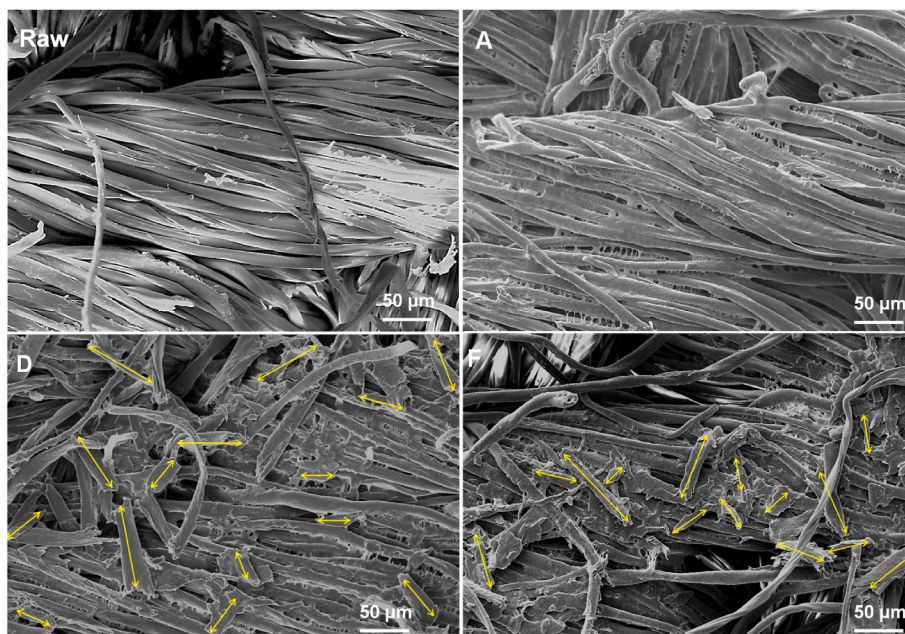


Fig. 8. SEM images of raw and printed fabrics in 500x magnification.

only added in the middle of the image, as there is no waste in the rest of the image, even some fibers cannot be covered by the printing paste. This result stems from the polar and hydrophilic nature of cellulosic waste particles that absorb printing paste by themselves and do not allow the rest of the fibers to be wetted. As mentioned before due to the high amount of waste particle inclusion (20%) in the sample of F, the printing paste is not adequate to completely wet the wastes, thus a non-uniform leveling of both printing paste and waste was observed on the fabric surface.

3.4. Surface wettability

Surface wettability characterizes the interaction between a surface and water molecules and is chiefly influenced by surface functionality.

Generally, functional groups on the surface increase surface energy, which is inversely proportional to contact angle values. The wettability character of a surface is also correlated to the surface polarity; less polarity means lower surface energies resulting higher contact angle values (Yu et al., 2015; Bouvet et al., 2016; Song et al., 2019). The contact angle values and images of water droplets on raw and screen-printed fabric surfaces can be observed in Fig. 10. Due to the hydrophilic nature of the cotton fabric, the least contact angle value of 91° was recorded on the raw fabric surface. After the application of the printing paste, the printed surface gained a hydrophobic nature thus the contact angle value increased to 141° . During the screen-printing process, the surface of the cotton fabric was coated by commercial acrylate and butadiene-based binders, and various auxiliaries which have less polarity compared to the hydroxyl functional cotton surface. As a result, the contact angle

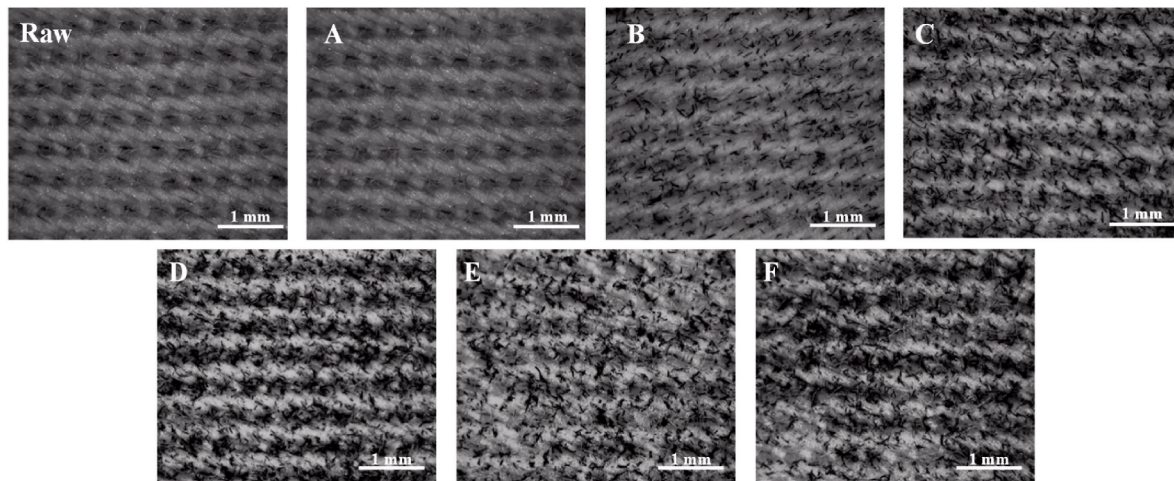


Fig. 9. Light microscopy images of raw and printed fabrics in 20x magnification.

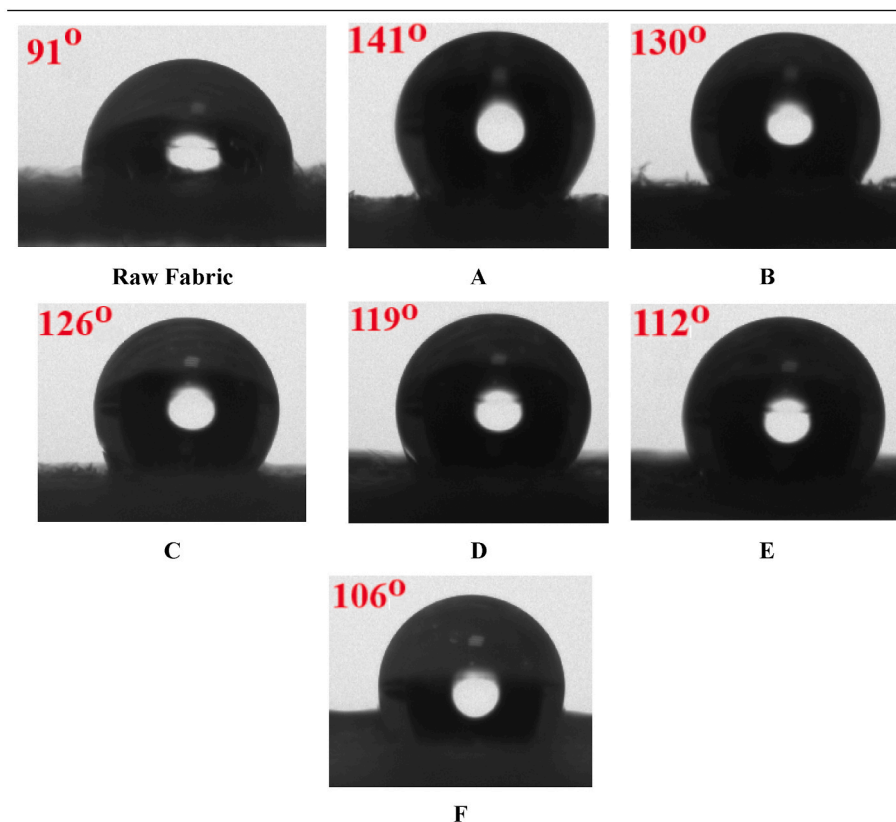


Fig. 10. Contact angle values and images of water droplets on raw and printed fabrics.

value increased in the sample of A compared to raw fabric. When the waste particles were included into the printing paste, the contact angle values were gradually decreased with increasing waste particle amount, due to the increment in surface functionality and polarity resulting in increase in surface energy.

3.5. Tensile properties

The tensile properties of the coated/printed textile materials are highly influenced by the rigidity/flexibility nature of the coating substrate (Mudri et al., 2020). Fig. 11 shows the tensile testing results of raw fabric and printed fabrics by means of tensile strength and elongation

values which were labeled as raw, A, B, C, D, E, and F. Accordingly, the highest extension value of 18.30% was recorded in the raw fabric. After the screen printing process, the sample of A, which has only printing paste on it, showed the least extension value of 13.31%. When the waste particles were included in the printing paste, the extension values varied in the range of 14.23–16.53 %. Considering the graph and numerical values, it is obvious that the extension of the printed fabrics decreased compared to the raw fabric. This result can be attributed to the rigid and brittle nature of the acrylate and butadiene-based binders which restricts the flexibility of cotton fiber resulting decline in extension. Considering the waste particle amounts, the extension values gradually increased with increasing waste amount in the screen-printing paste.

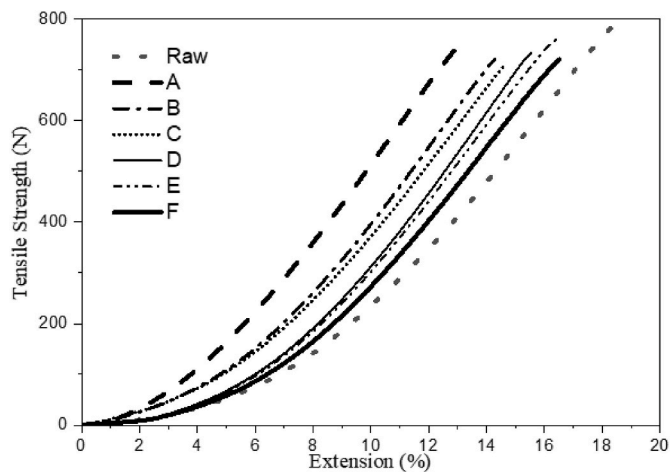


Fig. 11. Tensile strength and extension of the raw fabric and printed fabrics for each waste particle amount.

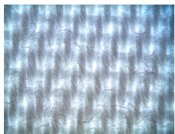
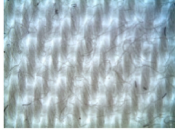




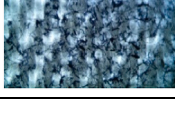
This result stems from the decline of the concentration of acrylate and butadiene-based polymeric cross-linkers in the paste. Considering the tensile strength values of samples, the highest breaking strength of 783 N was observed in the raw sample. The breaking strength of printed fabrics all decreased upon the application of the screen printing process and recorded in the range of 720–730 N. The sample of A, without any waste particle, showed the highest breaking strength value of 766 N among the other screen printed fabrics. There is no significant change recorded by means of the tensile strength values of printed fabrics including waste and the overall trend indicated a minor decrease compared to the breaking strength value of raw fabric. Previous studies have not investigated the tensile strength of waste particle printed textile fabrics. The only thing is that after the screen-printing process, the tensile strength value decreased for all fabrics compared to the raw fabric.

3.6. Air permeability

The air permeability of fabric is one of the clothing comfort properties and is mainly related to the voids between fiber/yarn intersections which are determined by the texture of the fabric, yarn counts/twist, existence of finishing/coating agents, etc. (Sarioğlu et al.; Matusiak, 2019). In this study, the air permeability test was employed to observe the effect of waste particle amount in screen printing paste on the air permeability property of screen-printed cotton fabrics. Table 2 shows the air permeability values of raw and printed fabrics for each waste particle amount. As expected the air permeability of raw fabric was significantly decreased after the screen printing process due to the existence of printing paste and waste particles which lower or partially cover the voids on the fabric surface (Çay et al., 2020). There is no great difference between the samples of A and B, which means the printing paste by itself also lowers the air permeability in such grades. Therefore, the inclusion of waste particles as colorants in the printing paste does not lead to a great loss in air permeability. Considering the samples of B to D, the air permeability value was gradually decreased with increasing waste particle amount in the printing paste. In the sample of E and F, although the waste particle amount increased, the air permeability increased. This result can be explained by the existence of a non-uniform printing layer on the sample of E and F due to the agglomeration of 15 and 20% of waste particles in the paste and the inefficacy of the liquid phase of the paste that is not completely covering the waste particles. This result can be also observed distinctly from the light microscopy fabric images in Table 2. The best uniform and homogeneous appearance was achieved in the sample of D with 10% waste particle inclusion.

Table 2

TS and air permeability values of raw and printed fabrics with light microscopy images.

Samples	TS750	SD	Air Permeability (L/min)	Macrostructure of the surfaces
Raw	98.4	0,30	23,5	
A	131.5	0,64	9	
B	141.2	0,77	8,5	
C	143.9	0,54	6,5	
D	149.1	0,56	6	
E	153.2	1,45	8	
F	176.5	1,83	10,5	

3.7. Handle properties

The handle properties of both the raw and printed fabrics were assessed using TSA, a method commonly used to evaluate the softness and smoothness of hygiene products and increasingly adopted in the textile industry. The measurement principle involves generating friction on the fabric surface using a rotating unit, resulting in sound vibrations at the fiber/fiber intersections, which are captured by a microphone. During testing, the signals at 750 Hz correspond to fabric smoothness, with a lower TS750 value indicating higher smoothness (Abu-Rous et al., 2017; Kim et al., 2021). Table 2 provides the TS and air permeability values of raw and printed fabrics with their light microscopy images from the surface. Accordingly, the raw fabric shows the least TS750 value, which represents the highest smoothness property, since there is no printing paste or waste particle on it. After the application of only printing paste, the TS750 value increased due to the existence of a polymeric layer with auxiliaries on the surface which are responsible for the roughness. As waste particles are incorporated into the printing paste, the surface roughness gradually increases with the greater quantity of waste particles in the paste. Considering the light microscopy images of the fabrics, due to the blue color of the waste particles, the blueness of the fabrics gradually and uniformly increased till sampling

D. Whereas, in samples E and F, the dispersion of the waste particles on the surface is not uniform, light and dark areas exist on the surface that is resulting from the agglomeration of the wastes above 10% inclusion. The SD values of samples E and F also support this result; higher SD means higher variations on the TS750 measurement.

4. Conclusions

In this study, the utilization of pre-consumed cellulosic textile wastes was achieved to contribute to sustainability by reusing and repurposing the textile wastes in a conventional screen-printing process. For this purpose, pre-consumed denim fabric wastes were converted into micron size and included in commercially available screen-printing pastes in various amounts. For the chemical characterization, FTIR, XRD, and EDS analysis were employed to observe the chemical changes on the printed fabric surfaces in terms of functional groups and crystallinity observation, respectively. The printed fabric properties such as color, washing/rub fastness, surface wettability, tensile, air permeability, and tactile properties were all examined to assess the impact of waste fibrous particle amount in the formulation. The dissipation performance of waste fibrous particles onto the fabric surfaces was also investigated by using light microscopy and SEM analysis.

When cellulosic waste fibrous particles were included in the printing paste, there were only minor alterations observed in the cotton fabric's chemical composition and crystallinity, according to the FTIR and XRD analysis. The addition of cellulosic waste particles, which were naturally crystalline, resulted in marginal increases in crystallinity up to 10 % waste inclusion. Above 10 % inclusions, the crystallinity started to decrease probably as a result of the agglomeration of wastes. The changes in elemental composition were evaluated by using EDS analysis based on the C/O atomic ratio. Among all printed fabrics, the highest C/O atomic ratio of 2.11 hence the highest solid add on value of 7.86 % were both recorded in the sample of D with a 10 % waste particle inclusion. Sample D was also determined as the optimal choice for color retention during washing and rubbing tests. Conversely, an excessive amount of waste particles (above 10 % waste inclusion) led to poor colorfastness, primarily due to agglomeration, creating an uneven printing surface. Light microscopy and SEM images supported also these results revealing the existence of agglomerated areas in the sample of F which consists of the highest waste content. The screen-printing process leads to a hydrophobic shift in surface wettability compared to the naturally hydrophilic cotton fabric. However, as the quantity of colored cellulosic waste fibrous particles increased, contact angle values decreased, by giving an enhanced surface functionality and reduced surface energy, which means better surface wettability. The inclusion of waste fibrous particles showed a linear relationship with decreased air permeability, with exceptions when agglomeration and non-uniform paste coverage occurred as in the samples of E and F. The TSA analysis of handle properties, focusing on fabric smoothness and softness, indicated that as waste particle content increased, the fabric's surface became progressively rougher. Notably, the non-uniform dispersed waste fibrous particles led to agglomeration, manifesting as light and dark areas on the fabric surface. Higher standard deviation values supported these observations. According to the tensile testing results, while elongation values gradually increased with higher waste particle amount in the printing paste, no substantial changes were observed in tensile strength values. This unique exploration of waste particle impact on comfort, including air permeability and tactile properties has provided valuable insights into the broader context of sustainable fabric printing. Therefore, this study will encourage further studies related to the tensile, visual, comfort properties, and usage performance of waste-printed textile fabrics in a sustainable manner. The balance between waste fibrous particle amount and end-product quality will be essential for the industry to adopt and benefit from this sustainable textile printing method.

CRedit authorship contribution statement

Zehra Yildiz: Writing – review & editing, Visualization, Methodology, Investigation. **Ilyas Kartal:** Writing – review & editing, Resources. **E. Dilara Kocak:** Writing – review & editing, Resources. **Berivan Ozer:** Writing – review & editing, Resources. **Betul Nur Kus:** Writing – review & editing, Resources. **Oguz Eryilmaz:** Writing – review & editing, Visualization, Methodology, Investigation.

Declaration of competing interest

The authors declare that they have no known competing financial interests or personal relationships that could have appeared to influence the work reported in this paper.

Data availability

Data will be made available on request.

References

- Abu-Rous, M., et al., 2017. A new physical method to assess handle properties of fabrics made from wood-based fibers. In: IOP Conference Series: Materials Science and Engineering. IOP Publishing.
- Ahmad, I., Kan, C.-w., Yao, Z., 2019. Photoactive cotton fabric for UV protection and self-cleaning. RSC Adv. 9 (32), 18106–18114.
- Al Faruque, M.A., et al., 2019. Preparation and characterisation of mechanically milled particles from waste alpaca fibres. Powder Technol. 342, 848–855.
- Al Faruque, M.A., et al., 2021. Graphene oxide incorporated waste wool/PAN hybrid fibres. Sci. Rep. 11 (1), 12068.
- Baysal, G., Kalav, B., Karagüzel Kayaoğlu, B., 2019. The effect of ultraviolet-curable water-borne polyurethane acrylate binder concentration on the printing performance of synthetic leather. Color. Technol. 135 (2), 111–120.
- Bouvet, G., et al., 2016. Impact of polar groups concentration and free volume on water sorption in model epoxy free films and coatings. Prog. Org. Coating 96, 32–41.
- Çay, A., et al., 2020. Application of textile waste derived biochars onto cotton fabric for improved performance and functional properties. J. Clean. Prod. 251, 119664.
- Cesar da Silva, P., et al., 2021. Evaluation of economic, environmental and operational performance of the adoption of cleaner production: survey in large textile industries. J. Clean. Prod. 278, 123855.
- Deniz, N.G., et al., 2022. Dyeing of polyester fibers with sulfur-and nitrogen-containing anthraquinone derivatives. Chem. Ind. Chem. Eng. Q. 28 (1), 47–55.
- Eryilmaz, O., Sancak, E., 2021. Effect of silane coupling treatments on mechanical properties of epoxy based high-strength carbon fiber regular (2 x 2) braided fabric composites. Polym. Compos. 42 (12), 6455–6466.
- Eryilmaz, O., Kocak, E.D., Sancak, E., 2023. 8 - braided natural fiber preforms. In: Midani, M., et al. (Eds.), Multiscale Textile Preforms and Structures for Natural Fiber Composites. Woodhead Publishing, pp. 221–237.
- Eryilmaz, O., et al., 2024. FEA and experimental ultimate burst pressure analysis of type IV composite pressure vessels manufactured by robot-assisted radial braiding technique. Int. J. Hydrogen Energy 50, 597–612.
- Gan, L., 2021. Production and Application of Fine Powder from Textile Waste. Deakin University.
- Gan, L., et al., 2021. Coloured powder from coloured textile waste for fabric printing application. Cellulose 28, 1179–1189.
- Idillovevna, S.M., 2023. Chemical composition OF plants and its analysis. International Journal of Pedagogics 3 (11), 165–170.
- Igini, M., Lam, C., 2023. 10 statistics about fast fashion waste [cited 2023 November 10th]; Available from: <https://earth.org/statistics-about-fast-fashion-waste/>.
- ISO 105-C06, 2010. Textiles - Tests for Colour Fastness - Part C06: Colour Fastness to Domestic and Commercial Laundering.
- ISO 105-X12, 2016. Textiles - Tests for Colour Fastness - Part X12: Colour fastness to Rubbing.
- ISO 13934-1, 2013. Textiles — Tensile Properties of Fabrics — Part 1: Determination of Maximum Force and Elongation at Maximum Force Using the Strip Method.
- ISO 9237, 1999. Textiles - Determination of Permeability of Fabrics to Air.
- Kibasomba, P.M., et al., 2018. Strain and grain size of TiO₂ nanoparticles from TEM, Raman spectroscopy and XRD: the revisiting of the Williamson-Hall plot method. Results Phys. 9, 628–635.
- Kim, H.J., et al., 2021. Indexing surface smoothness and fiber softness by sound frequency analysis for textile clustering and classification. Textil. Res. J. 91 (1–2), 200–218.
- Kumar, A., Sharma, M., Vaish, R., 2022. Screen printed calcium fluoride nanoparticles embedded antibacterial cotton fabric. Mater. Chem. Phys. 288, 126449.
- Kutanaee, H.N., 2011. Perpetration of styrene-butadiene acrylate anti bacterial binders and their application on cotton/polyester printing. Afr. J. Microbiol. Res. 5, 1842–1849.
- Määttänen, M., et al., 2021. Pre-treatments of pre-consumer cotton-based textile waste for production of textile fibres in the cold NaOH (aq) and cellulose carbamate processes. Cellulose 28, 3869–3886.

- Matusiak, M., 2019. Moisture Management Properties of Seersucker Woven Fabrics of Different Structure. *Fibres & Textiles in Eastern Europe*.
- Mudri, N.H., et al., 2020. Comparative study of aromatic and cycloaliphatic isocyanate effects on physico-chemical properties of bio-based polyurethane acrylate coatings. *Polymers* 12 (7), 1494.
- Nam, S., et al., 2016. Segal crystallinity index revisited by the simulation of X-ray diffraction patterns of cotton cellulose I β and cellulose II. *Carbohydrate polymers* 135, 1–9.
- O Connell, J., et al., 2016. Characterization of crystallite morphology for doped strontium fluoride nanophosphors by TEM and XRD. *Phys. B Condens. Matter* 480, 169–173.
- Patti, A., Cicala, G., Acierno, D., 2020. Eco-sustainability of the textile production: waste recovery and current recycling in the composites world. *Polymers* 13 (1), 134.
- Rajkhowa, R., et al., 2012. Ultrafine wool powders and their bulk properties. *Powder Technol.* 224, 183–188.
- Sarioğlu, E., et al., Investigation of effect of pre-consumer recycling acrylic fiber ratio on yarn and fabric properties. *Int. J. Mater. Eng. Technol.* 5(2): p. 91-96.
- Savageau, A.E., 2011. Textile Waste and Sustainability: a Case Study. *Research Journal of Textile and Apparel*.
- Sheikh, J., Bramhecha, I., Teli, M., 2015. Recycling of terry towel (cellulosic) waste into carboxymethyl cellulose (CMC) for textile printing. *Fibers Polym.* 16, 1113–1118.
- Song, K., et al., 2019. Interaction of surface energy components between solid and liquid on wettability, and its application to textile anti-wetting finish. *Polymers* 11 (3), 498.
- Tang, W., et al., 2022a. Fine powders from dyed waste wool as odor adsorbent and coloration pigment. *Powder Technol.* 400, 117261.
- Tang, W., et al., 2022b. Porous, colorful and gas-adsorption powder from wool waste for textile functionalization. *J. Clean. Prod.* 366, 132805.
- Tayyab, M., et al., 2020. A sustainable development framework for a cleaner multi-item multi-stage textile production system with a process improvement initiative. *J. Clean. Prod.* 246, 119055.
- Tseghai, G.B., et al., 2020. Development of a flex and stretchy conductive cotton fabric via flat screen printing of PEDOT: PSS/PDMS conductive polymer composite. *Sensors* 20 (6), 1742.
- Wang, F., et al., 2019. Synthesis and properties of in-situ bulk high impact polystyrene toughened by high cis-1, 4 polybutadiene. *Polymers* 11 (5), 791.
- Yasin, S., Sun, D., 2019. Propelling textile waste to ascend the ladder of sustainability: EOL study on probing environmental parity in technical textiles. *J. Clean. Prod.* 233, 1451–1464.
- Yasukawa, A., Fukuyama, M., Iwai, K., 2021. Dyeing silk and cotton fabrics using Fuji apple peel and the properties of the dyed fabrics. *Textil. Res. J.* 91 (21–22), 2669–2681.
- Yildiz, Z., Onen, H.A., 2017. Dual-curable PVB based adhesive formulations for cord/rubber composites: the influence of reactive diluents. *Int. J. Adhesion Adhes.* 78, 38–44.
- Yildiz, Z., Eryilmaz, O., 2023. 12 - Preimpregnated natural fiber preforms. In: Midani, M., et al. (Eds.), *Multiscale Textile Preforms and Structures for Natural Fiber Composites*. Woodhead Publishing, pp. 327–340.
- Yousef, S., et al., 2019. A new strategy for using textile waste as a sustainable source of recovered cotton. *Resour. Conserv. Recycl.* 145, 359–369.
- Yousef, S., et al., 2020. Sustainable green technology for recovery of cotton fibers and polyester from textile waste. *J. Clean. Prod.* 254, 120078.
- Yu, Y., et al., 2015. Synthesis and characterization of photosensitive-fluorosilicone–urethane acrylate prepolymers. *Des. Monomers Polym.* 18 (3), 199–209.